npj | vaccines

Article

Published in partnership with the Sealy Institute for Vaccine Sciences

https://doi.org/10.1038/s41541-025-01346-z

# Next-generation mRNA vaccines eliciting robust protection against multidrug-resistant *Enterobacteriaceae*



Rui Liu[1,3], Shi Xu[2,3], Shang Liu[2,3], Mengwei Xu[2], Jing Li[2], Aili Wang[2], Wei Li[2], Lingzhi Zhan[2], Keyue Ruan[2], Caiyi Fei[2], Zengding Wu[2], Tiyun Han[2] ✉ & Yafei Cai[1] ✉

Antibiotics are essential for treating bacterial infections, but the growing problem of antimicrobial resistance (AMR) undermines their effectiveness. Vaccines targeting multidrug-resistant (MDR) bacteria are urgently needed. Here, we developed next-generation mRNA vaccines encoding two novel target antigens: phosphate-specific transport protein (PstS) and DUF3748 domain-containing protein (YidR). The resulting fusion proteins exhibited high expression and secretion in vitro and provided strong protective efficacy in mice against *Klebsiella pneumoniae (K. pneumoniae)* and *enterohemorrhagic Escherichia coli* (EHEC), significantly reducing bacterial loads and organ damage. Moreover, the *K. pneumoniae*-based mRNA vaccine (KV3), encoding the PstS-YidR fusion protein, elicited notable cross-protection against four *Enterobacteriaceae* species, including *K. pneumoniae*, EHEC, *Salmonella enterica* (*S. enterica*), and *Shigella flexneri* (*S. flexneri*). In conclusion, this study demonstrates the potential of mRNA vaccines employing fusion protein containing a novel target antigen to combat MDR *Enterobacteriaceae* with significant cross-protective effects.

Bacterial infections remain one of the major threats to global public health, contributing to high morbidity and numerous complications worldwide. Clinically, antibiotics are primarily used to treat and suppress bacterial infections and remain the most effective form of treatment to date[1]. However, the rapid rise of antimicrobial resistance (AMR) has rendered many antibiotics ineffective, leading to persistent infections and increased healthcare costs[2]. The World Health Organization (WHO) has identified multidrug-resistant (MDR) *Klebsiella pneumoniae* (*K. pneumoniae*), *Escherichia coli* (*E. coli*), and *Salmonella* as critical pathogens that urgently require new treatment strategies[3]. Members of the *Enterobacteriaceae* family, including *E. coli*, *K. pneumoniae*, and *Salmonella*, etc., can cause intestinal, pulmonary, and urinary tract infections. These pathogens account for a significant proportion of both hospital- and community-acquired infections, particularly in immunocompromised individuals and those with underlying health conditions[4,5]. For example, *K. pneumoniae* and *E. coli* are major causes of urinary tract infections, pneumonia, and sepsis[5,6]. In contrast, *Salmonella* species are associated with foodborne illness and enteric fever[7]. This alarming trend highlights the urgent need for alternative strategies to combat bacterial infections, with preventive vaccines emerging as a promising solution.

Effective vaccines have been developed against *Streptococcus pneumoniae* (*S. pneumoniae*) and *Haemophilus influenzae* type B, significantly reducing the global burden of these infections[8]. However, prophylactic vaccines for *K. pneumoniae*, *E. coli*, and *Salmonella* etc., remain limited despite their substantial clinical impact. Current vaccine strategies for bacterial infections include live-attenuated vaccines, inactivated whole-cell vaccines, subunit vaccines, conjugate vaccines, and toxoid vaccines[9]. Among these, live-attenuated vaccines can elicit robust cellular and humoral immune responses but pose safety concerns due to the potential risk of reversion in immunocompromised hosts[10]. Subunit vaccines target specific bacterial components, such as outer membrane proteins or capsular polysaccharides, to induce an immune response[11]. Polysaccharide conjugate vaccines have demonstrated efficacy against encapsulated bacteria such as *S. pneumoniae* but offer limited cross-protection against diverse bacterial strains[12]. The currently available typhoid conjugate vaccine (TCV) provides protection against typhoid fever but is ineffective against non-typhoidal *Salmonella* infections such as *Salmonella enteritidis*[13]. To date, no licensed vaccines are available for *K. pneumoniae* or *E. coli* and related pathogens, underscoring the urgent need for novel vaccine approaches.

The rapid development and successful application of mRNA-based vaccines against SARS-CoV-2 have highlighted the potential of this

[1]College of Animal Science and Technology, Nanjing Agricultural University, Nanjing, China. [2]Nanjing Chengshi (TheraRNA) Biomedical Technology Co. Ltd., Nanjing, China. [3]These authors contributed equally: Rui Liu, Shi Xu, Shang Liu. ✉e-mail: hantiyun@therarna.cn; ycai@njau.edu.cn

platform for combating bacterial infections[14,15]. mRNA vaccines offer several advantages over conventional vaccine platforms, including rapid development, high immunogenicity, the ability to encode multiple antigens simultaneously, and no requirement for additional adjuvants[16]. These vaccines rely on lipid nanoparticle (LNP) delivery systems to enhance antigen presentation and stimulate robust immune responses[17]. Recent studies have demonstrated that mRNA vaccines encoding bacterial antigens can induce protective immunity. For example, mRNA vaccines encoding PcrV or OprF-I elicited strong immune responses and provided broad protection against *Pseudomonas aeruginosa* (*P. aeruginosa*) infections in mice[18]. Similarly, a multivalent mRNA vaccine targeting toxins and virulence factors protected animals against *Clostridioides difficile* infections across multiple models[19]. However, developing broadly protective mRNA vaccines against diverse bacterial serotypes remains challenging due to the high variability of bacterial antigens[20,21]. Therefore, selecting highly conserved antigens or combining multiple antigens to create multivalent vaccines is currently considered one of the most effective strategies for providing cross-protection against MDR bacterial infections[22].

Recent research has identified several promising vaccine targets within MDR *Enterobacteriaceae*. The DUF3748 domain-containing protein (YidR), for instance, is highly conserved and expressed across multiple MDR strains, including *K. pneumoniae* and *E. coli*[23,24]. YidR has been shown to mediate bacterial adhesion and invasion and may also play a role in bacterial stress response and biofilm formation, making it an attractive target for vaccine development[23]. An mRNA-based vaccine targeting YidR combined with the *K. pneumoniae* tissue plasminogen activator (tPA) signal sequence conferred broad protection in lung infection models[25]. Nonetheless, identifying additional conserved target antigens with effective neutralizing epitopes remains critical for developing prophylactic vaccines with broader protective effects.

The reverse vaccinology approach has previously been used to identify conserved antigens from extensive clinical isolates[26]. One such candidate is the phosphate-specific transport protein (PstS), which plays a vital role in bacterial survival under phosphate-limiting conditions. The PstS protein vaccine induces protective humoral responses against MDR *Salmonella Pullorum* infections in poultry[26]. Reports indicate that PstS is primarily located in the bacterial periplasm and embedded in the outer membrane[27]. In certain MDR bacteria, PstS expression has been associated with the production of virulence factors involved in biofilm formation and host cell adhesion[28]. Previous studies have verified that PstS protein-based vaccines are effective against bacterial infections in poultry. However, it remains unclear whether PstS confers similar protection in mammals. This suggests that the conserved PstS antigen may have potential as a broad-spectrum protective vaccine target against MDR *Enterobacteriaceae* infections in mammalian hosts.

In this study, we developed next-generation mRNA vaccines targeting the PstS protein—a novel antigen for bacterial infection in mammals—fused with YidR. Preliminary construction of the mRNA vaccines (KV3 and EV3) demonstrated high expression and secretion in vitro. These two prophylactic mRNA vaccines effectively protected mice infected with *K. pneumoniae* and *enterohemorrhagic E. coli* (EHEC), respectively. Sequence alignment analysis revealed high homology of PstS and YidR among *K. pneumoniae*, EHEC, *Salmonella enterica* (*S. enterica*), and *Shigella flexneri* (*S. flexneri*). Furthermore, the *K. pneumoniae*-based KV3 vaccine provided cross-protection against all four pathogens. In contrast, no protective effect was observed against *Proteus mirabilis* (*P. mirabilis*), which exhibited low sequence homology. The vaccine's impact on the intestinal microbiota diversity of mice was only temporary, and the microbiota soon returned to normal.

## Results

### PstS-containing mRNA vaccines exhibit prophylactic effect against *K. pneumoniae* infection

PstS is a component of the bacterial phosphate-specific transport (Pst) system, located in the periplasmic space and possessing a high affinity for phosphate[27]. To date, no prophylactic vaccine targeting PstS for preventing MDR *Enterobacteriaceae* infections in mammals has been reported. Additionally, the conserved YidR antigen, known to play roles in bacterial infection and biofilm formation, has been recognized as a promising vaccine target[28]. *K. pneumoniae* is among the most drug-resistant pathogens within the *Enterobacteriaceae* family[29]. Therefore, we first developed three mRNA vaccine constructs based on PstS alone and its fusion with YidR in a *K. pneumoniae* challenge model (Fig. 1a). To enhance antigen trafficking and stability, the Fc domain of human immunoglobulin heavy chain constant region γ1 protein (IGHG1) and STABILON (Stab) elements were incorporated into the mRNA constructs[30,31] (Fig. 1a). Analysis of mRNA integrity showed that the purities of KV1 (PstS), KV2 (YidR-PstS), and KV3 (PstS-YidR) ranged from 88.0% to 90.0% (Supplementary Fig. 1a). In vitro expression assays confirmed successful expression of both single-antigen and fusion-antigen constructs (Fig. 1b and Supplementary Fig. 2). KV1 exhibited the highest secretion ratio into the supernatant. Although KV2 and KV3 displayed similar secretion levels, KV3 showed a lower intracellular proportion, indicating higher secretion efficiency. Considering the importance of antigen secretion for stimulating humoral immunity, KV1 and KV3 were selected for in vivo testing. The prepared mRNA-LNPs demonstrated uniform size distribution, distinct surface charges, and high encapsulation efficiencies (Supplementary Fig. 1b, c).

As shown in Fig. 1c, mice were immunized twice and subsequently challenged intranasally with *K. pneumoniae*. Lung tissues were collected to evaluate bacterial load and pathological changes. Compared to the phosphate-buffered saline (PBS) control group, mice immunized with KV1 and KV3 experienced less weight loss, though the difference was not significant (Fig. 1d). Vaccinated groups, especially KV3, showed significantly reduced bacterial loads in the lung tissue (Fig. 1e, f). Quantitative analysis revealed that bacterial loads decreased by approximately 18-fold with KV1 and 180-fold with KV3 (Fig. 1f). Histological analysis (Fig. 1g) showed that untreated infected mice had thickened alveolar septa and disrupted alveolar structure with extensive inflammatory infiltration. KV1-immunized mice showed partially thickened septa with moderate infiltration, while KV3-immunized mice maintained better alveolar structure with minimal inflammation, indicating superior protection. These results suggest that mRNA vaccines encoding PstS or PstS-YidR fusion antigens can effectively prevent *K. pneumoniae* lung infections in mice.

### PstS-containing mRNA vaccines provide prophylactic protection against EHEC infection

MDR *E. coli* is one of the most common commensal bacteria in the intestines of humans and animals. However, polysaccharide vaccines currently under investigation offer only limited cross-protection[32]. Therefore, we selected EHEC, one of the most pathogenic strains within the *Enterobacteriaceae* family, to develop three mRNA vaccine constructs based on PstS and its fusion with YidR (Fig. 2a). These constructs were designated EV1 (PstS), EV2 (PstS-mutation YidR), and EV3 (PstS-truncation-mutation YidR). In EV2 and EV3, mutations were introduced at specific YidR amino acid sites to prevent glycosylation in mammalian cells. Further truncation in EV3 (PstS-truncation-mutation YidR) aimed to improve the expression efficiency of the fusion antigen. Quality control analysis showed that the purities of the three mRNAs were 90.3%, 88.5%, and 88.0%, respectively (Supplementary Fig. 3a). As shown in Fig. 2b and Supplementary Fig. 4, all three constructs were successfully expressed and secreted in vitro. EV1 exhibited significantly higher secretion levels than the other constructs. Additionally, the EV2 construct was predominantly expressed intracellularly, while EV3 displayed more balanced intracellular expression and secretion. Therefore, EV1 and EV3, with relatively greater secretion capacity, were selected for subsequent animal studies. Characterization of the mRNA-LNPs demonstrated uniform particle distribution and positive surface charge (Supplementary Fig. 3b, c).

Mice were immunized and challenged as illustrated in Fig. 2c. The bacterial loads in the colon and ileum of vaccinated mice were significantly

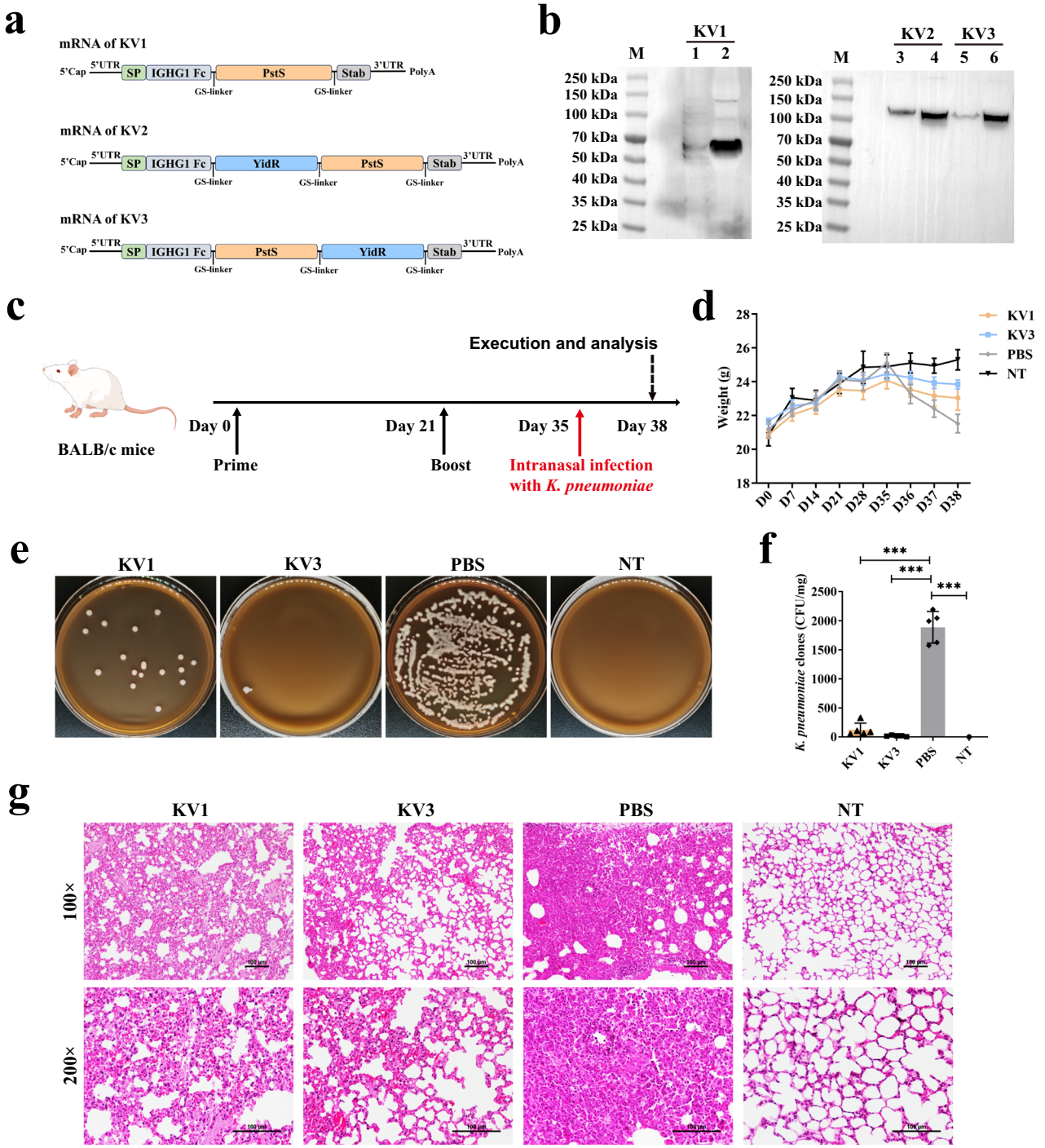


**Fig. 1 | Development, expression and prophylactic effect of mRNA vaccines against *K. pneumoniae*.** **a** Schematic of mRNA construct in developed mRNA vaccines against *K. pneumoniae* infection. **b** Western blotting (WB) analysis of antigens expressed in HEK293T transfected with the indicated mRNA and marker (M), cell proteins (lines 1, 3, and 5), and supernatants (lines 2, 4, and 6) are shown in the panel. **c** Schematic of vaccination with mRNA vaccines in BALB/c mice and intranasal infection with *K. pneumoniae*. **d** Weight change of mice with different treatments throughout the experiment. Bacterial load assay including **e** representative captures and **f** average amount of bacterial clones in LB medium, and **g** pathological analysis by H&E staining for lung tissue from different groups of mice. Representative results are in **f** presented as means ± standard deviation (SD). The differences among multiple groups were analyzed by one-way *ANOVA* with Tukey's multiple comparisons test. This approach was chosen to evaluate differences among more than two normally distributed groups while controlling for type I error. Values of *** $p < 0.001$ were considered significant.

lower than those of PBS-immunized controls, by approximately 75%–80% (Fig. 2d, e). Pathological analysis of the colon showed that intestinal villi in the non-treated (NT) group remained structurally intact, with no significant lesions or inflammatory infiltration. In contrast, PBS-injected mice displayed extensive inflammatory cell infiltration in the submucosa and severe damage to the villi, including fragmentation and lysis (Fig. 2f). However, vaccinated mice exhibited markedly reduced pathological changes. These findings suggest that the mRNA vaccines based on PstS and the PstS-truncation-mutation YidR fusion antigen can effectively prevent EHEC infection.

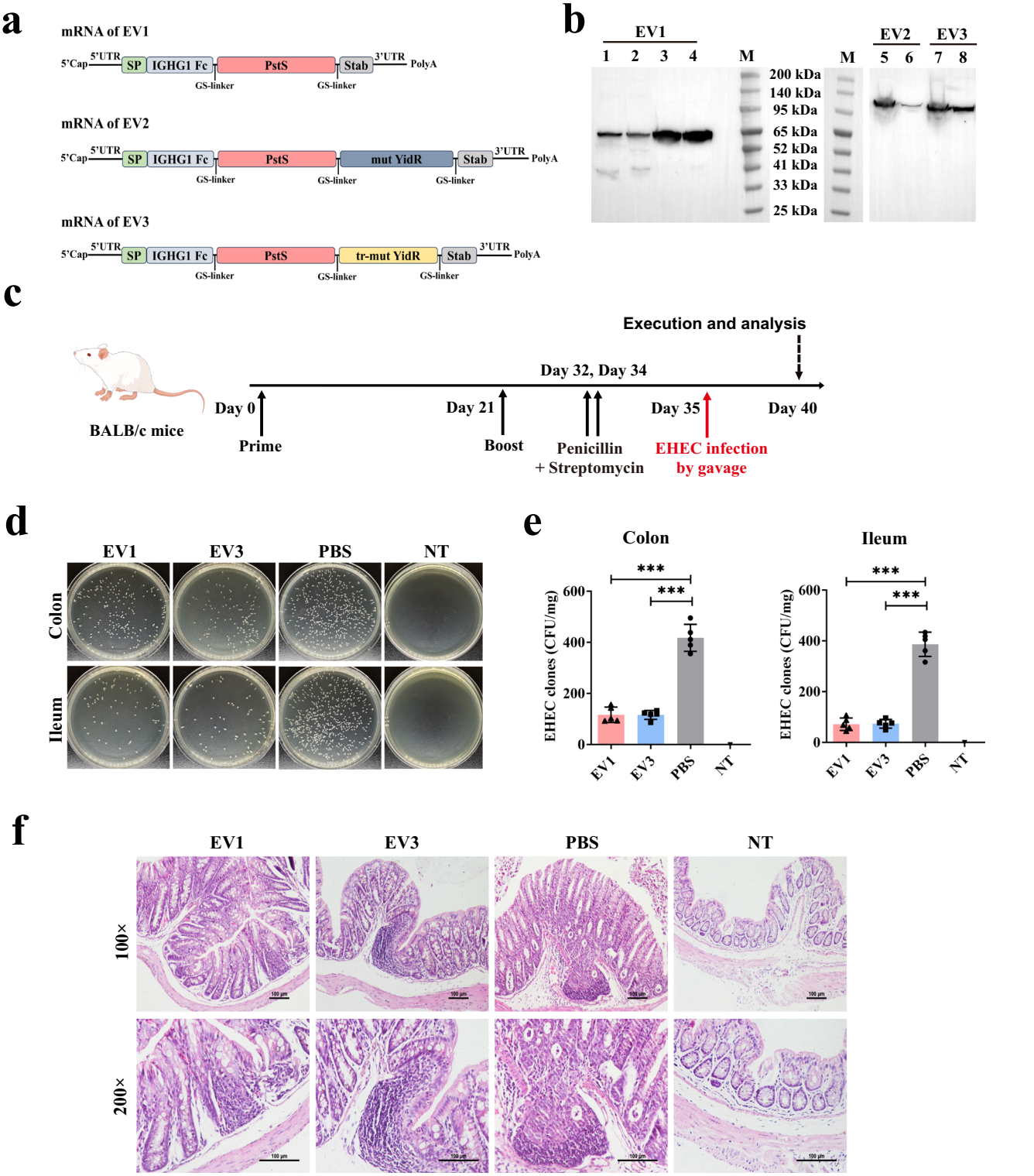


**Fig. 2 | Development, expression and prophylactic effect of mRNA vaccines against EHEC. a** Schematic of mRNA construct in developed mRNA vaccines against EHEC infection. **b** WB analysis of antigens expressed in HEK293T transfected with the indicated mRNA and marker (M), cell proteins (lines 1, 2, 5, and 7), and supernatants (lines 3, 4, 6, and 8) are shown in the panel. **c** Schematic of vaccination with mRNA vaccines in BALB/c mice, antibiotic treatment, and EHEC infection by gavage. Bacterial load assay including **d** representative captures and **e** average amount of bacterial clones in LB medium for colon and ileum from different groups of mice, and **f** pathological analysis by H&E staining for colon. Representative results are presented as means ± SD. The differences among multiple groups were analyzed by one-way *ANOVA* with Tukey's multiple comparisons test. This approach was chosen to evaluate differences among more than two normally distributed groups while controlling for type I error. Values of *** $p < 0.001$ were considered significant.

### PstS-containing mRNA vaccines are effective in protecting against *S. enterica* infection

Similar to *E. coli*, *S. enterica* resides in the intestine and can cause infections when the immune system is compromised or prolonged antibiotic use leads to dysbiosis[33]. Currently, prophylactic vaccines against *S. enterica* infections remain under investigation, and no vaccine targeting PstS or YidR for *S. enterica* has yet been reported. Accordingly, we developed two vaccine constructs, SV1 and SV2, based on PstS and PstS-YidR, respectively (Fig. 3a). The purities of the two prepared mRNAs were 90.1% and 88.1%, respectively (Supplementary Fig. 5a). In vitro expression results confirmed that both mRNAs were expressed and secreted, with SV1 (PstS-YidR) exhibiting a higher secretion level (Fig. 3b and Supplementary Fig. 6). Both constructs were tested in vivo, and Supplementary Fig. 5b, c show the diameter distribution, ZP, and encapsulation efficiency following formulation.

Bacterial load and pathological analyses were conducted after mice were immunized and infected as illustrated in Fig. 3c. Unlike the results observed with the previous two bacterial infection models, Fig. 3d, e show that SV1-immunized mice had significantly lower *S. enterica* loads in feces, spleen, and liver, whereas SV2 did not demonstrate a similar effect. Hematoxylin and eosin (H&E) staining of the jejunum revealed abnormal morphology and disrupted intestinal villi in the mucosal layer of PBS-immunized mice and those immunized with SV2. These mice also showed extensive tissue damage and inflammatory cell infiltration or hemorrhage near the central celiac blood vessels. In contrast, mice immunized with SV1 exhibited significantly fewer inflammatory cells and reduced intestinal tissue damage (Fig. 3f). Additionally, the reduction of splenic microsomes in vaccinated mice was alleviated. These findings indicate that an mRNA vaccine targeting only the PstS antigen can effectively protect against *S. enterica* infection and minimize tissue damage. However, the mRNA construct encoding the PstS-YidR antigen did not show prophylactic effects. This may be attributed to reduced secretion efficiency or an unstable structure following antigen fusion (Fig. 3b).

### mRNA vaccine encoding conserved PstS and YidR antigens exhibit cross-protective effect against multiple MDR *Enterobacteriaceae* infections

Based on the above results, mRNA vaccines encoding PstS-containing antigens from each genus significantly induced protective effects in three bacterial challenge experiments. Interestingly, previous research has shown that immunization with recombinant YidR protein from *K. pneumoniae* can reduce *E. coli* infection in cows[24]. This raised the question of whether a single mRNA sequence could be developed to generate an mRNA vaccine effective against multiple MDR *Enterobacteriaceae* species. This possibility is supported by the high conservation of these antigens among MDR bacteria.

To investigate whether PstS could serve as a broad-spectrum vaccine target against multiple MDR *Enterobacteriaceae* infections, we retrieved the amino acid sequences of the PstS protein expressed by five MDR *Enterobacteriaceae* species and performed sequence homology analyses. The results revealed that PstS shared high sequence homology among four species (*K. pneumoniae*, *E. coli*, *S. enterica*, and *S. flexneri*), with over 89% identity. Notably, *S. enterica* and *E. coli* displayed 100% identity for a partial sequence, while *P. mirabilis* exhibited less than 80% similarity compared to the other four species (Supplementary Fig. 7). To further enhance the cross-protective effect of the mRNA vaccine, YidR was also analyzed. The sequence homology of YidR was slightly lower than that of PstS, with more than 78% identity among the four bacteria, but only 55–57% identity in *P. mirabilis* (Supplementary Fig. 8).

Based on the above analysis, we next verified whether KV3 (PstS-YidR), developed in the *K. pneumoniae* challenge experiment (Fig. 4a), could exert a preventive effect against multiple *Enterobacteriaceae* species. First, analysis of antibody titers showed that high levels of PstS-specific IgG and moderate levels of YidR-specific IgG were produced following prime-boost vaccination (Fig. 4b). Furthermore, lung bacterial load analysis demonstrated that KV3 provided strong protection against *K. pneumoniae* infection, with significant improvements in lung inflammation, alveolar structure integrity (Fig. 4c–e). KV3 also effectively inhibited EHEC infection in the intestines of mice, alleviating intestinal villus damage and inflammatory cell infiltration in the colon (Fig. 4f–h). In the *S. enterica* infection model, KV3 markedly reduced bacterial loads in the intestine, spleen, and liver and significantly lessened organ damage (Fig. 4i–k), indicating a different protective effect compared to SV2.

Further analysis in the *S. flexneri* infection model (Fig. 5a) confirmed that intestinal bacterial infection was still effectively inhibited by KV3 (Fig. 5b–d). The vaccine also reduced inflammatory cell infiltration in the colonic mucosa, slowed damage progression of the intestinal epithelial structure, and mitigated injury to the glomerular basement membrane and tubular dilation in the kidneys. Additionally, KV3 alleviated weight loss in mice caused by all four of the above bacterial infections, providing effective protection (Supplementary Fig. 9a–d). However, KV3 did not confer preventive protection in the *P. mirabilis* infection model (Fig. 5e–g and Supplementary Fig. 9e). We speculate that this lack of protection is likely related to the lower sequence homology of PstS and YidR in *P. mirabilis* compared to the other MDR *Enterobacteriaceae* species, suggesting that the vaccine lacks effective antigenic epitopes against *P. mirabilis* infection.

### mRNA vaccine has minimal impact on the diversity of intestinal microbiota in mice

Studies have shown that some commensal *Enterobacteriaceae* bacteria colonize the gut microbiota of humans and mice[34]. To assess whether KV3, which targets multiple pathogenic MDR *Enterobacteriaceae* infections, affects the diversity of commensal gut microbiota, we performed 16S rRNA sequencing and analyzed fecal microbiota diversity at different time points during mouse immunization (Fig. 6a). Analysis of α- and β-diversity revealed that although gut microbiota diversity fluctuated on days 7 and 28 post-immunization, it returned to pre-immunization levels by day 42 (Fig. 6b, c). Changes in species richness at the phylum level showed that on days 7 and 28, the relative proportion of *Firmicutes* increased in some mice, while that of *Bacteroidetes* decreased (Fig. 6d). Similarly, family-level analysis indicated that *Lachnospiraceae* abundance significantly increased and *Muribaculaceae* abundance decreased during immunization (Fig. 6e); however, both returned to baseline levels by day 42. Finally, the relative abundance of the *Enterobacteriaceae* family and the *Escherichia-Shigella* genus (Fig. 6f, g) did not show significant changes at any time point. Additionally, alignment analysis of PstS from *K. pneumoniae* and the five main commensal gut bacterial families at baseline (day 0) confirmed the absence of homology, further supporting the minimal likelihood of vaccine-induced cross-reactivity (Supplementary Fig. 10). These findings indicate that KV3 has only a temporary impact on the intestinal microbiota diversity of mice, which soon recovers to normal conditions.

## Discussion

Current preventive vaccines for many MDR bacteria affecting humans and domestic animals remain inadequate. Excessive antibiotic use has further accelerated bacterial resistance and increased infection risks[5,6]. Existing preventive vaccine strategies primarily rely on live-attenuated strains, inactivated whole-cell vaccines, conjugate vaccines, subunit vaccines, or toxoid vaccines. However, these approaches generally fail to provide broad immunoprotection and rarely achieve cross-protection against multiple bacterial subtypes[12]. The MDR *Enterobacteriaceae* family includes species such as *K. pneumoniae*, *E. coli*, *S. enterica*, *S. flexneri*, and *P. mirabilis*, etc., for which no licensed vaccines are currently available. This study identified PstS as a promising new target for developing a prophylactic mRNA vaccine against four *Enterobacteriaceae* infections in mammals.

The development of bacterial vaccines centers on stimulating specific humoral and cellular immune responses to achieve bacterial clearance[9,35]. Humoral immunity eliminates bacteria through antibody binding, opsonization, and biofilm disruption, while cellular immunity mediates the clearance of intracellular bacteria via activated antigen-presenting cells

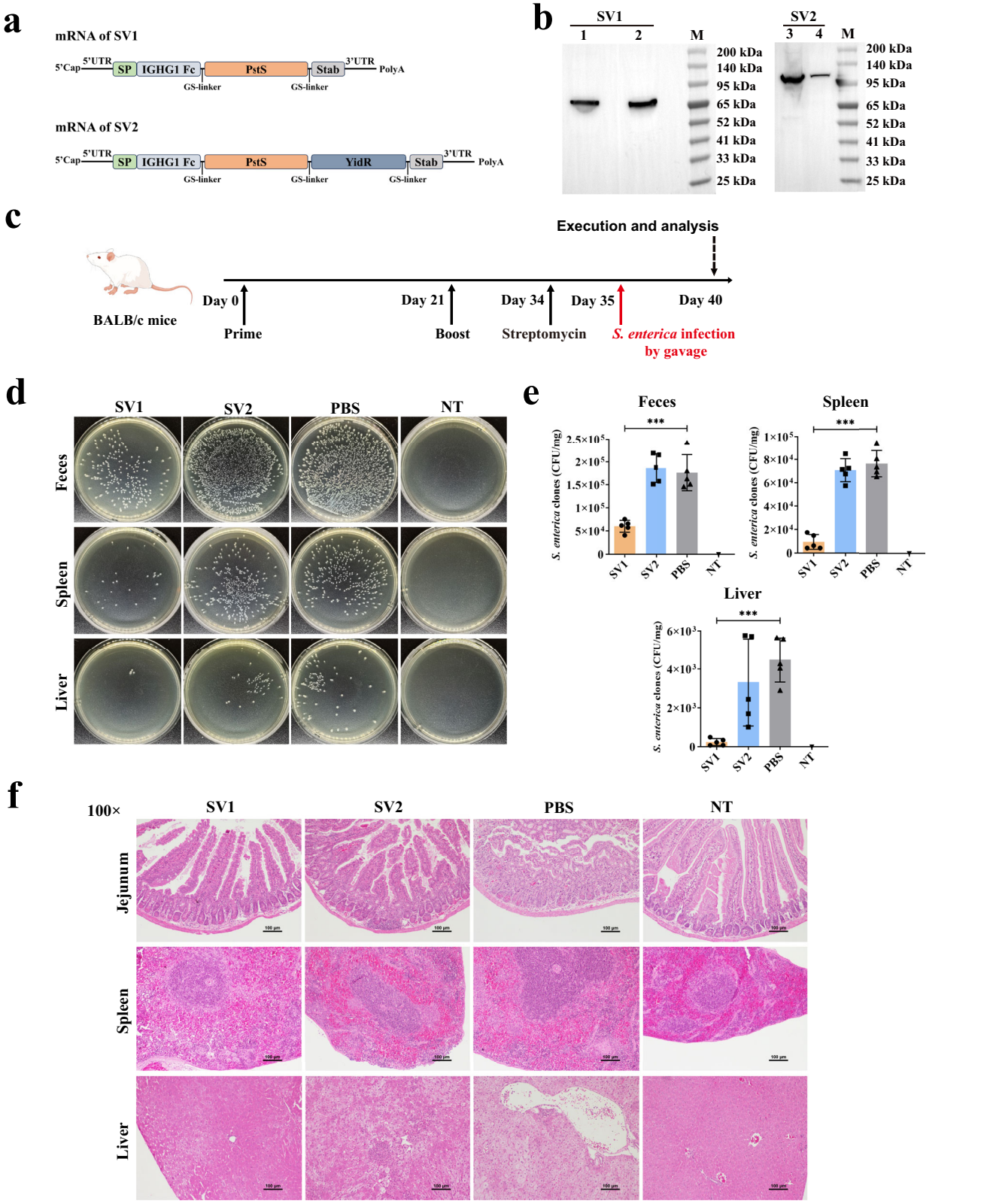


**Fig. 3 | Development, expression and prophylactic effect of mRNA vaccines against *S. enterica*.** **a** Schematic of mRNA construct in developed mRNA vaccines against *S. enterica* infection. **b** WB analysis of antigens expressed in HEK293T transfected with the indicated mRNA and marker (M), cell proteins (lines 1 and 3) and supernatants (lines 2 and 4) are shown in the panel. **c** Schematic of vaccination with mRNA vaccines in BALB/c mice, streptomycin treatment and gavage infection with *S. enterica*. Bacterial load assay for feces, spleen, and liver from different groups of mice, including (**d**) representative captures and **e** average amount of bacterial clones in LB medium. **f** Pathological analysis by H&E staining of jejunum, spleen, and liver. Representative results are presented as means ± SD. The differences among multiple groups were analyzed by one-way *ANOVA* with Tukey's multiple comparisons test. This approach was chosen to evaluate differences among more than two normally distributed groups while controlling for type I error. Values of $^{***}p < 0.001$ were considered significant.

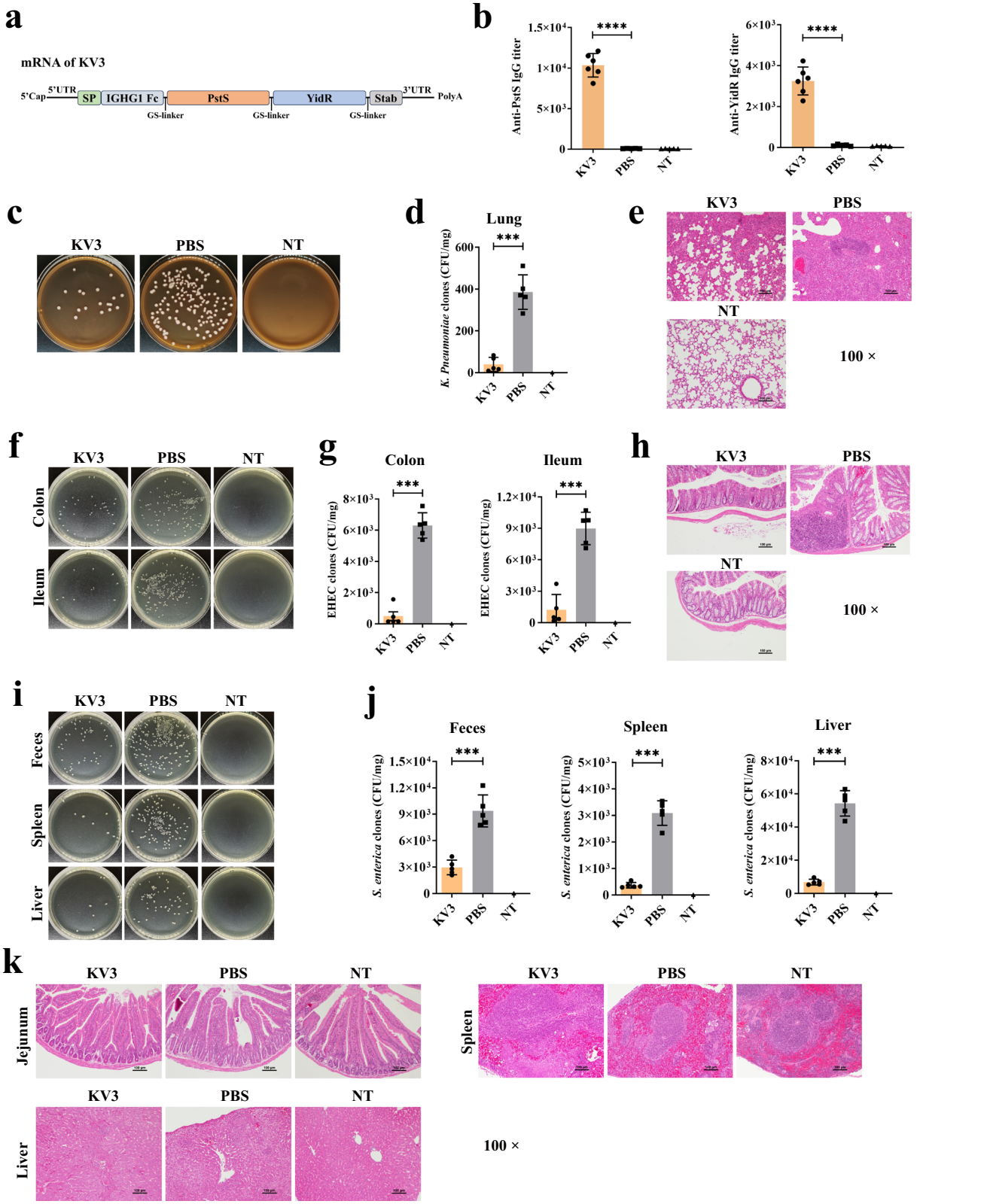


**Fig. 4 | Prophylactic effect of KV3 against *K. pneumoniae, EHEC and S. enterica*.** **a** Schematic of mRNA construct in selected KV3 based on sequence of PstS and YidR antigens from *K. pneumoniae*. The prophylactic effect analysis in *K. pneumonia* was conducted using **b** Serum IgG antibody titer analysis against the PstS or YidR antigen on day 28 after prime-boost vaccination. **c**, **d** bacterial load assay and **e** pathological analysis for lung tissue from different groups of mice. The prophylactic effect analysis in EHEC was conducted using **f**, **g** bacterial load assay for colon and ileum from different groups of mice, and **h** pathological analysis for colon. The prophylactic effect analysis in *S. enterica* was conducted using **i**, **j** bacterial load assay for feces, spleen, and liver from different groups of mice, and **k** pathological analysis for jejunum, spleen, and liver. Representative results are presented as means ± SD. The differences among multiple groups were analyzed by one-way *ANOVA* with Tukey's multiple comparisons test. This approach was chosen to evaluate differences among more than two normally distributed groups while controlling for type I error. Values of $***p < 0.001$ and $****p < 0.0001$ were considered significant.

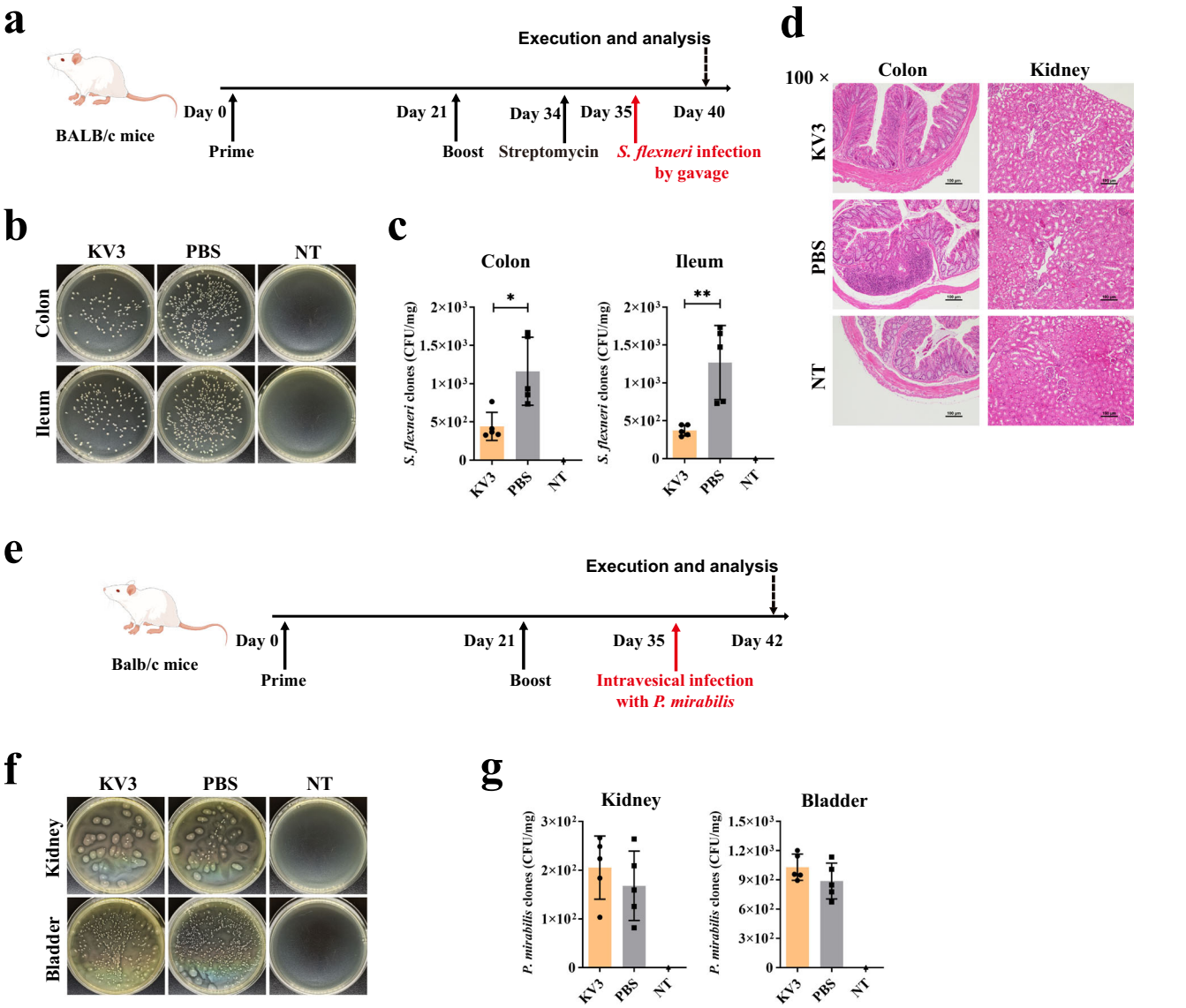


**Fig. 5 | Prophylactic effect of KV3 against *S. flexneri and P. mirabilis*.** **a** Schematic of vaccination with KV3 in BALB/c mice, streptomycin treatment and *S. flexneri* infection by gavage. **b**, **c** Bacterial load assay for colon and ileum from KV3-vaccinated and *S. flexneri*-infected mice, and **d** pathological analysis for colon and kidney. **e** Schematic of vaccination with KV3 in BALB/c mice and intravesical infection with *P. mirabilis*. **f**, **g** Bacterial load assay for kidney and bladder from different groups of mice. Representative results are presented as means ± SD. The differences among multiple groups were analyzed by one-way *ANOVA* with Tukey's multiple comparisons test. This approach was chosen to evaluate differences among more than two normally distributed groups while controlling for type I error. Values of $^{*}p < 0.05$ and $^{**}p < 0.01$ were considered significant.

(APCs) and T cells[36,37]. For instance, live-attenuated vaccines mimic natural infections and activate both humoral and cellular immunity, producing durable memory responses[38]. In contrast, pneumococcal vaccines primarily depend on T-independent B-cell responses, which generate relatively weak immune memory[39]. Subunit vaccines, such as the acellular pertussis (aP) vaccine, promote Th2-skewed humoral immunity through aluminum-based adjuvants[40]. Unlike these traditional platforms, mRNA vaccines can activate cytotoxic T lymphocytes (CTLs) through endogenous antigen expression. Our mRNA vaccines were designed based on the conserved antigens PstS and YidR, differing from conventional capsular polysaccharide or subunit vaccines. KV3 induced strong antibody titers against PstS, while the response to YidR was comparatively lower. This difference may be attributed to fusion-mediated structural effects that reduced the exposure of antibody-neutralizing epitopes.

This study primarily evaluated the humoral immune response triggered by the PstS-YidR mRNA vaccine, as well as the correlation between the prophylactic effect and serum IgG titers. The effective protection against bacterial infections, particularly those involving facultative intracellular pathogens such as *S. enterica* and *S. flexneri*, also depends on cellular immune mechanisms[41]. Although the cellular immunity induced by the PstS-YidR mRNA vaccine was not evaluated in this study, other mRNA vaccines targeting bacteria have focused on it. For example, Huang et al. reported that YidR mRNA vaccines combined with tPA signal sequence elicit both humoral response and Th1-biased immune response against *K. pneumoniae*[25]. Wang et al. found that PcrV or OprF-I mRNA vaccine candidates elicited a mixed Th1/Th2 or slighted Th1-biased immune response and conferred protection against *P. aeruginosa* infection[18]. Considering the limitation in cellular immunity research, future research should include analyses of cytokine profiles and T-cell activation to determine whether the vaccine also triggers cellular immune responses that contribute to bacterial clearance.

Selecting appropriate target antigens is critical for determining vaccine efficacy, specificity, and the type of immune response induced. Developing bacterial vaccines with cross-protective capability remains particularly

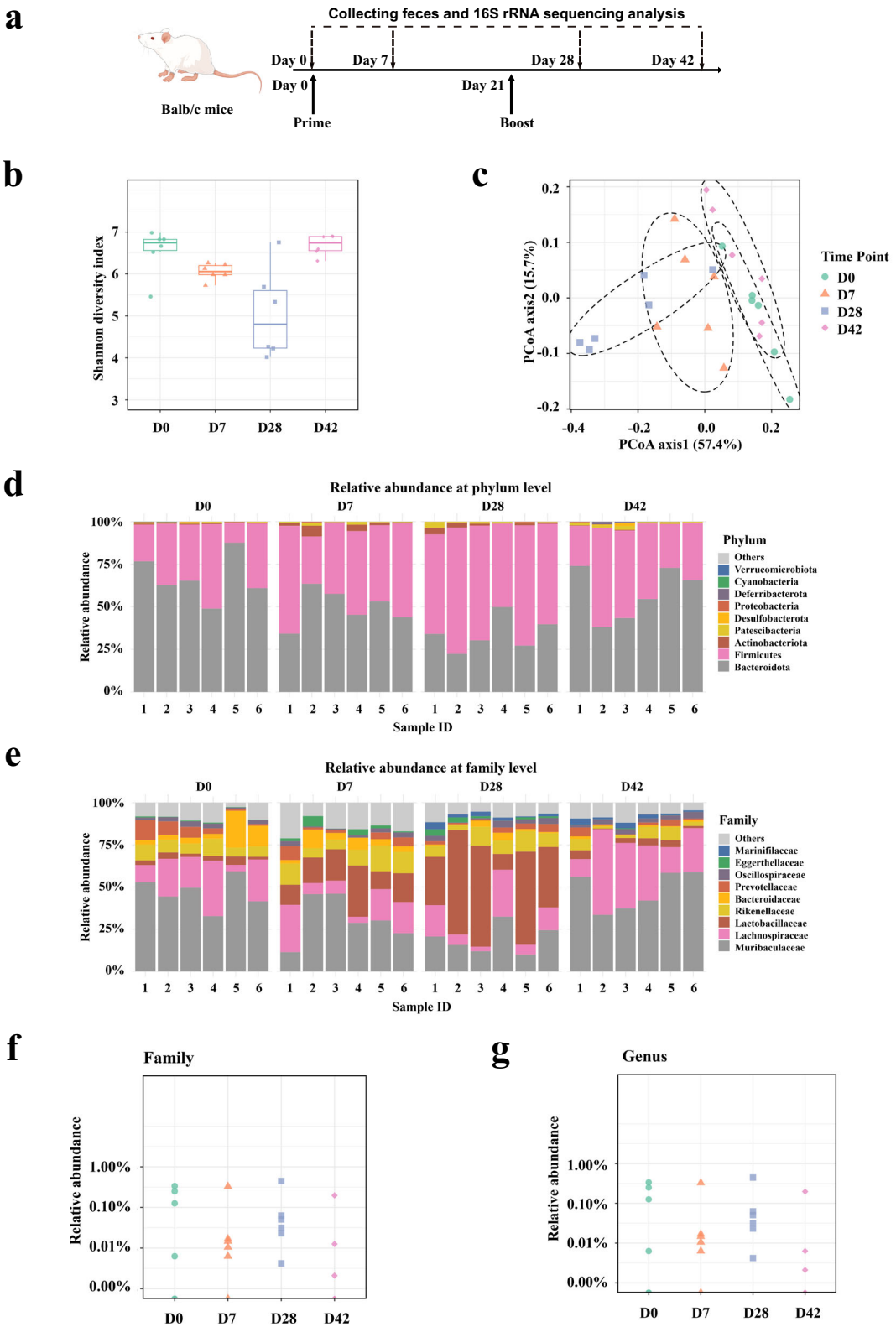


**Fig. 6 | Analysis of changes in intestinal microbiota diversity before and after immunization with mRNA Vaccines. a** Schematic of the vaccination process using KV3 in BALB/c mice, as well as a 16S rRNA sequencing analysis at different timepoints. **b** The α-diversity analysis indicated by Shannon diversity index plots. **c** The β-diversity analysis indicated by principal coordinates analysis (PCoA). The relative abundances at **d** the phylum and **e** the family levels at different timepoints. Relative abundances of **f** *Enterobacteriaceae* family and **g** *Escherichia–Shigella* genus at different timepoints. Each dot represents a unique sample from each experimental group (color) taken at different timepoint following vaccination (shape).

challenging due to the vast diversity of bacterial species and subtypes[39]. For example, *K. pneumoniae* can be divided into 82 capsular serotypes, among which K1, K2, and K5 are closely associated with severe human and animal infections[42]. Current strategies for broad-spectrum bacterial vaccines generally focus on conserved and multivalent antigens across different species. Using mRNA platforms, multivalent vaccines have been designed to provide cross-protection against multiple bacterial pathogens[22]. In this study, we developed fusion mRNA vaccines based on conserved PstS and YidR antigens. The vaccine effectively cross-protected against four *Enterobacteriaceae* infections but did not prevent *P. mirabilis* infection. This lack of protection likely reflects the lower sequence homology of PstS and YidR in *P. mirabilis* compared with the other species.

In multivalent vaccine design, maintaining stable three-dimensional conformations of fusion proteins is essential for efficient expression, secretion, and enhanced immunogenicity through the presentation of multiple antigenic epitopes[43]. The configuration of fusion antigens can influence both protein folding and expression efficiency. In this study, we incorporated the Fc domain of IGHG1 and STABILON elements into the constructs and truncated effective antigen fragments to improve stability[30,31]. In vitro expression results showed that the PstS-YidR mRNA constructs (KV3 and EV3) were efficiently expressed and secreted, providing strong protection against *K. pneumoniae* and EHEC infections, respectively. These findings suggest that PstS and YidR from these two bacteria maintain stable conformations and do not interfere with each other's expression. In contrast, the fused construct (SV2), which combined PstS and YidR, impaired protein expression and secretion. This resulted in a lack of protection in the *S. enterica* infection model. We speculate that YidR fusion from *S. enterica* may alter the secretion efficiency of PstS in SV1 or destabilize the protein structure in the supernatant. Conversely, SV1 demonstrated excellent protective efficacy, likely due to its stable expression and secretion. Thus, optimizing protein conformation through truncation, mutation, or alternative fusion strategies may further enhance protective efficacy. Additionally, the fusion mRNA vaccine KV3, developed in the *K. pneumoniae* challenge model, also inhibited *S. enterica* infection and pathology, indicating a cross-protective effect. This observation is consistent with the previously reported cross-protection mediated by YidR from *K. pneumoniae* against *E. coli* infection[24].

The choice of vector and adjuvant also significantly influences immune potency and response levels[44]. In addition to traditional live-attenuated and subunit vaccines, DNA vaccines, VLP vaccines, and nanocarrier-based vaccines are being actively explored for bacterial prophylaxis. For instance, antigen delivery using engineered exosomes or VLPs can enhance immunogenicity[45,46]. Various adjuvants are also under investigation for bacterial protein vaccines[44]. In our study, the antigen-encoding mRNA was delivered using a safe LNP vector (SM102 LNP). Both the LNP and the mRNA possess intrinsic immune-activating properties, allowing them to act as self-adjuvants. Future strategies that optimize delivery systems and improve antigen presentation—such as through membrane-based delivery platforms—could further enhance vaccine efficacy.

Although our 16S rRNA sequencing analysis revealed only transient changes in the gut microbiota following KV3 vaccination, this conclusion is limited by the short observation period and the use of a single mouse model. In future research, additional experimental animal models, such as other mammals, can be employed to monitor changes in commensal bacteria or other immune-related responses over a longer observation period. Importantly, the amino acid sequence of PstS used in our vaccine was selected from the *Enterobacteriaceae* family and is conserved among *Enterobacteriaceae*. In addition, previous studies have shown that *Enterobacteriaceae* typically constitute less than 1% of the healthy gut microbiota[47]. This low abundance likely contributes to the limited impact of vaccination on commensal bacterial populations. Furthermore, homology analysis between *K. pneumoniae* and the five major commensal gut bacterial families in mice indicated that there is almost no possibility of cross-reactivity for the PstS antigen. Nevertheless, a comprehensive evaluation of commensal microbiota safety should be considered in future studies.

This study presents an innovative mRNA vaccine strategy for combating MDR *Enterobacteriaceae*. mRNA vaccines encoding PstS alone or fused with YidR demonstrated high efficiency in protecting against various *Enterobacteriaceae* infections. Then, a conservation analysis was employed to select antigens from *K. pneumoniae* for developing mRNA vaccines with cross-protective potential. The vaccine ultimately exhibited protective effects against several *Enterobacteriaceae* bacteria. Importantly, the mRNA-based bacterial vaccine technology could reduce antibiotic dependence and lower the incidence of nosocomial infections caused by MDR pathogens. Moreover, the flexibility and rapid adaptability of this platform make it a promising candidate for future translational applications against emerging bacterial threats.

In conclusion, we developed a next-generation mRNA vaccine encoding the novel antigen PstS, along with the conserved YidR antigen. Both antigens were successfully expressed and secreted in vitro. The mRNA vaccine containing the conserved PstS-YidR fusion sequence demonstrated cross-protective effects against four MDR *Enterobacteriaceae* infections, while showing only a temporary impact on intestinal microbiota diversity. This study provides a new antigen target and vaccine design strategy for the development of broad-spectrum prophylactic vaccines against MDR *Enterobacteriaceae*, laying the groundwork for future clinical research on bacterial infection prevention in humans and animals.

## Methods

### Study design

A series of experiments was conducted to evaluate the expression, immunogenicity, and protective efficacy of mRNA vaccines developed to prevent bacterial infections. First, vaccines expressing PstS and YidR from *K. pneumoniae* were developed and tested for anti-infective protection using a mouse lung infection model. Next, vaccines expressing the same types of antigens from EHEC were constructed and evaluated for immunoprotective effects in a mouse gastrointestinal infection model. Mutations were introduced into the YidR antigen of EV2 (PstS–mutation YidR) at specific amino acid residues to prevent glycosylation in mammalian cells. To further enhance expression efficiency, a truncated version of the fusion antigen—designated EV3 (PstS-truncation-mutation YidR)—was generated. Subsequently, two mRNA vaccines encoding PstS and YidR antigens from *S. enterica* were constructed and compared for their protective efficacy in a gastrointestinal infection model in mice. Finally, based on amino acid sequence homology analyses of PstS and YidR across five MDR *Enterobacteriaceae* species (*K. pneumoniae*, *E. coli*, *S. enterica*, *S. flexneri*, and *P. mirabilis*), a multivalent *Enterobacteriaceae* mRNA vaccine with broad-spectrum protection was designed using *K. pneumoniae*-derived PstS and YidR sequences and tested for protective efficacy against these pathogens.

### Plasmid construction

The pUC57 vector was used for in vitro transcription (IVT) of mRNA and for plasmid construction. A T7 promoter element was introduced to enable efficient IVT. The vector contained 5′- and 3′-untranslated regions (UTRs) and a 110-nucleotide poly(A) tail to enhance mRNA stability and translation efficiency. Each construct included antigen sequences fused at the N-terminus to the IGHG1 and a flexible GGS linker (GGSGGSGGSG). The C-terminus contained a GS linker (GSGSGSG), Stab element, and 6×His tag for improved stability and detection. For different vaccine constructs, antigen variants—with or without truncations or mutations—were cloned into the appropriate vector sites. All antigen-coding sequences were codon-optimized for high expression efficiency, and the DNA was synthesized by GenScript. The plasmids were validated by restriction enzyme digestion and Sanger sequencing to ensure the integrity of the inserts and regulatory elements.

### mRNA synthesis

Template plasmids were linearized by restriction digestion for IVT. The IVT reaction was performed using linearized plasmids and the MEGAscript® T7 Transcription Kit (Thermo Fisher Scientific) with a modified protocol. The

resulting mRNA was capped at the 5′ end with a trinucleotide Cap1 analogue (CleanCap, N-7413, TriLink). After a 6-h incubation and DNA template degradation, IVT products were purified by lithium chloride precipitation. mRNA concentration and purity were measured using a NanoDrop spectrophotometer (Thermo Fisher Scientific, USA), and integrity was confirmed by capillary electrophoresis. The final mRNA products were stored at 4 °C for short-term use.

### mRNA-LNP preparation

The mRNA was encapsulated in SM-102 LNP using a microfluidic system. SM-102, 1,2-distearoyl-sn-glycero-3-phosphocholine (DSPC), cholesterol, and polyethylene glycol (PEG) 2000-dimyristoylglycerol (DMG) were dissolved in ethanol at a molar ratio of 50:10:38.5:1.5. The mRNA samples were diluted in 20 mM sodium acetate buffer (pH 5.5) to the desired final concentration. The aqueous and organic phases were combined in a microfluidic mixing chip at a flow rate ratio of 95:5. The lipid-to-mRNA weight ratio was approximately 25:1, enabling spontaneous self-assembly of positively charged lipids with negatively charged mRNA. The resulting mRNA–LNPs were neutralized to pH 7.0–7.4 with 1 M Tris-HCl (pH 8.0), filtered through a 0.22 μm membrane, and stored at 2–8 °C. Particle size, polydispersity index (PDI), and zeta potential (ZP) were measured using dynamic light scattering (DLS). Encapsulation efficiency was determined using the Quant-iT RiboGreen RNA Quantification Kit (R11490, Thermo Fisher Scientific) according to the manufacturer's protocol.

### In vitro expression of mRNA

HEK293T cells were seeded in 6-well plates at a density of $8 \times 10^5$ cells per well in MEM Basal Medium (11095080, Gibco) supplemented with 10% fetal bovine serum (FBS). To assess expression and secretion, naked mRNA was transiently transfected using LNP3[48], a lipid nanoparticle–based delivery system optimized for efficient mRNA transfection. After 48 h, cell supernatants and lysates were collected. Cells were lysed with RIPA buffer to obtain total protein. Protein concentrations were measured using the BCA assay, followed by Western blotting (WB) to detect antigen expression levels.

### Western blotting

Each protein sample (40 μg) was mixed with 5× loading buffer, vortexed, and heated at 100 °C for 5 min, followed by centrifugation at 12,000 rpm for 5 min at 4 °C. Proteins were separated by sodium dodecyl sulfate–polyacrylamide gel electrophoresis (SDS-PAGE) and transferred onto PVDF membranes. Membranes were blocked with 5% skim milk at room temperature (RT) for 1 h and incubated overnight at 4 °C with a His-tag rabbit polyclonal antibody (LF308, Epizyme Biotech, Shanghai, China) diluted 1:1000 in General Antibody Diluent (PS119L, Epizyme Biotech). After three washes with Tris-buffered saline containing Tween-20 (TBST), membranes were incubated with horseradish peroxidase (HRP)–conjugated goat anti-rabbit IgG (H + L) (LF102, Epizyme Biotech) diluted 1:5000 in TBST for 1 h at RT. Membranes were washed three times with TBST and visualized using Omni-ECL Enhanced Detection Reagent (SQ101L, Epizyme Biotech) with a ChemiDoc™ imaging system (Bio-Rad, USA).

### Animals

All mice were obtained from Charles River Laboratories (Beijing, China). All experimental procedures were approved and conducted in accordance with the *Guidelines for the Care and Use of Laboratory Animals* published by the U.S. National Institutes of Health. The animals were housed under controlled environmental conditions with 50%–60% relative humidity and a 12-h light/dark cycle. Food and water were provided ad libitum. All procedures complied with national and institutional ethical standards for laboratory animal welfare.

### Culturing and preparing bacteria for infection

**K. pneumoniae (ATCC 13883)**. The lyophilized bacterial powder was thawed at −80 °C and resuspended in 1 mL of sterile PBS. The suspension was mixed thoroughly and streaked onto Columbia blood agar plates using a sterile inoculating loop. Plates were incubated at 37 °C for 24 h. A single colony was transferred to Todd–Hewitt Broth supplemented with yeast extract (THY medium) and incubated at 37 °C for 24 h. The bacterial suspension was then diluted 1:1000 and re-inoculated into fresh THY broth for another 24-h incubation at 37 °C. The culture was centrifuged at 4000 rpm for 10 min, and the supernatant was discarded. The pellet was resuspended in sterile PBS, and the bacterial concentration was adjusted to $2 \times 10^8$ CFU/mL.

**EHEC (CICC 24187) and *S. enterica* (ATCC 13311)**. The lyophilized bacterial stocks were thawed separately at −80 °C, resuspended in 1 mL of sterile PBS, and mixed thoroughly. Each strain was streaked onto Luria–Bertani (LB) agar plates and incubated at 37 °C for 18 h. A single colony was transferred to LB broth and incubated at 37 °C for 24 h. The bacterial suspensions were then adjusted to $2 \times 10^9$ CFU/mL for EHEC and $2 \times 10^7$ CFU/mL for *S. enterica* using sterile physiological saline.

***S. enterica* (ATCC 29903)**. The lyophilized powder was thawed at −80 °C and resuspended in 1 mL of sterile PBS. The bacteria were streaked onto nutrient agar plates using a sterile inoculating loop and incubated at 37 °C for 24 h. A single colony was transferred into nutrient broth and incubated at 37 °C for 24 h. The culture was diluted 1:1000 into fresh nutrient broth and incubated for another 24 h at 37 °C. The bacterial suspension was centrifuged at 4000 rpm for 10 min, the supernatant was removed, and the pellet was resuspended in sterile physiological saline. The final bacterial concentration was adjusted to $2 \times 10^6$ CFU/mL.

**P. mirabilis (CMCCB49005)**. The lyophilized bacterial powder was thawed at −80 °C, resuspended in sterile PBS, and mixed thoroughly. The bacteria were streaked onto tryptic soy agar (TSA) plates and incubated at 37 °C for 24 h. A single colony was transferred into tryptic soy broth (TSB) and incubated for further amplification. The bacterial concentration was adjusted to $1 \times 10^9$ CFU/mL using sterile physiological saline.

### Vaccination and bacterial infection

Female BALB/c mice (6–8 weeks old, 18–25 g) were randomly assigned to ensure the equitable distribution ($n = 5$). A total of 135 mice were used for the following infection experiments:

**For K. pneumoniae infection**. Mice were vaccinated subcutaneously in the left groin with PBS, KV1 (PstS), or KV3 (PstS-YidR) at a dose of 100 μL (5 μg) on days 0 and 21. On day 35, mice were intranasally challenged with 50 μL ($1 \times 10^7$ CFU) of *K. pneumoniae* (ATCC 13883) following overnight fasting.

**For EHEC infection**. Mice received PBS, EV1 (PstS), or EV3 (PstS-truncation–mutation YidR) vaccines in the same manner. A penicillin–streptomycin mixture was administered by gavage on days 32 and 34, followed by oral infection with 500 μL ($1 \times 10^9$ CFU) of EHEC (CICC 24187) on day 35.

**For *S. enterica* infection**. Mice were vaccinated with PBS, SV1 (PstS-LpfB), or SV2 (PstS-YidR) as above. Streptomycin was administered by gavage on day 34, followed by oral infection with 500 μL ($1 \times 10^7$ CFU) of *S. enterica* (ATCC 13311) on day 35.

**Cross-protection analysis**. To evaluate cross-protection, mice were vaccinated with PBS or KV3 following the same schedule. The vaccinated mice were then challenged with *K. pneumoniae*, EHEC, or *S. enterica* as described above. For *S. flexneri* infection: KV3 was administered as described, followed by streptomycin gavage on day 34. On day 35, mice were orally infected with 500 μL ($1 \times 10^6$ CFU) of *S. flexneri* (ATCC 29903). For *P. mirabilis* infection: KV3 was injected subcutaneously as

described. On day 35, mice were intravesically infected with 50 μL ($5 \times 10^7$ CFU) of *P. mirabilis* (CMCCB49005).

In all challenge experiments, an NT group that received neither vaccination nor infection served as a control. Prior to *K. pneumoniae* or *P. mirabilis* infection, mice were briefly anesthetized with 1%–3% isoflurane in an induction chamber to facilitate rapid bacterial administration. No anesthesia was required for the other infections. After infection, mice were maintained under standard housing conditions and monitored daily for body weight, appearance, and behavior.

### Tissue collection and analysis

On days 38, 40, or 42, mice were euthanized by intraperitoneal injection of an overdose of pentobarbital sodium (150 mg/kg), in accordance with institutional ethical protocols. Tissues for bacterial load quantification and histopathology were selected according to each pathogen's infection route and tissue tropism: For *K. pneumoniae*, lungs were collected to assess pulmonary colonization and inflammation. For EHEC, the ileum and colon were analyzed as the primary colonization sites and the colon was analyzed as lesion site. For *S. enterica*, feces, spleen, and liver were collected to evaluate intestinal colonization and systemic dissemination; jejunum, spleen, and liver were used for histopathological assessment. For *S. flexneri*, colon and ileum were analyzed as primary infection sites, while colon and kidney sections were examined for systemic pathology. For *P. mirabilis*, bladder and kidney were collected to represent the ascending urinary tract infection pathway. Tissues were rinsed with PBS and fixed in 4% paraformaldehyde for H&E staining. Additional tissue or fecal samples were collected for bacterial load quantification.

### Serum and gut microbiota analysis

For antibody titer analysis in *K. pneumoniae* challenge experiments, serum samples were collected on day 28 after the prime-boost KV3 vaccination. To assess intestinal microbiota composition, mice were immunized with KV3 on days 0 and 21 using the same procedure. Fecal samples were collected aseptically and cryopreserved on days 0, 7, 28, and 42. Samples were sent to Novogene (Beijing, China) for 16S rRNA sequencing and microbial community analysis.

### Bacterial load assay for tissue and feces

At the end of each animal experiment, infection-related tissues or fecal samples were collected aseptically from each mouse group. Approximately 10 mg of each sample was weighed and transferred into sterile tubes containing 100 μL of sterile PBS. Tissues were homogenized on ice using a mechanical tissue homogenizer until no visible debris remained. The homogenates were then diluted 1:100 with sterile PBS. After thorough mixing, 100 μL of each diluted sample was spread evenly onto the following agar plates: Columbia blood agar for *K. pneumoniae*, LB agar for EHEC and *S. enterica*, nutrient agar for *S. flexneri*, and TSA for *P. mirabilis*. Five replicate plates were prepared for each sample to ensure accuracy. The selected media were optimized for each bacterial species to support robust growth and produce distinctive colony morphology, facilitating differentiation from residual commensal flora. Assessment of background flora levels was carried out using plates inoculated with samples from uninfected control mice (some of which had been treated with antibiotics). The absence of colonies on these plates confirmed the absence of infection or contamination. All plates were incubated at 37 °C for 48 h. The bacterial colonies were then counted and photographed for record keeping.

### Indirect enzyme-linked immunosorbent assay for antibody titers

Serum levels of PstS- or YidR-specific IgG were quantified using an indirect enzyme-linked immunosorbent assay (ELISA). Briefly, 96-well microplates were coated overnight at 4 °C with recombinant PstS or YidR antigens, which had been expressed and purified from *E. coli*. After three washes with PBST, each well was blocked with 3% bovine serum albumin (BSA) for 2 h at RT. Following blocking, the plates were washed again, and 100 μL of serially diluted serum samples were added per well. The plates were incubated for 2 h at RT with gentle agitation. After washing three times, 100 μL of HRP-conjugated rabbit anti-mouse IgG antibody (diluted 1:5000) was added to each well and incubated for another 2 h at RT under gentle shaking. After the final washing step, 100 μL of 3,3′,5,5′-tetramethylbenzidine (TMB) substrate solution (6602ES60, Yeasen) was added to each well and allowed to react for 15 min at RT in the dark. The reaction was terminated with 50 μL of 2 M $H_2SO_4$ per well. Absorbance was measured at 450 nm using a microplate reader (Multiskan FC, Thermo Fisher Scientific).

### Protein sequence alignment analysis

Full-length amino acid sequences of PstS or YidR from *K. pneumoniae*, *E. coli*, *S. enterica*, *S. flexneri*, *P. mirabilis*, and five commensal gut bacteria were retrieved from the UniProt database. Sequence alignment analyses were performed separately for each protein using the ESPript 3.0 web tool (https://doi.org/10.1093/nar/gku316). Additionally, sequence homology analyses of PstS and YidR across the bacterial species were performed using the Align tool on the UniProt website to determine sequence similarity values for these target antigens.

### 16S rRNA sequencing analysis

Fecal sample sequencing was performed according to standard procedures established at Novogene (Beijing, China). Genomic DNA was extracted using a commercial extraction kit, and the V3-V4 regions of the 16S rRNA gene were amplified with specific primers. The PCR products were sequenced using the Illumina NovaSeq platform. Raw sequencing data were processed using QIIME2 for quality control, operational taxonomic unit (OTU) clustering, and taxonomic assignment based on the 16S rRNA reference database. Downstream data analyses were conducted in the R statistical environment. α- and β-diversity indices were calculated to evaluate microbial community composition and intergroup differences. Relative abundances at the phylum, family, and genus levels were compared among the groups.

### Statistical analysis

The differences between the two groups were compared via the unpaired *Student's t*-test. The differences among multiple groups were analyzed by one-way analysis of variance (*ANOVA*) with Tukey's multiple comparisons test. Values of $^*p < 0.05$, $^{**}p < 0.01$, $^{***}p < 0.001$, and $^{****}p < 0.0001$ were considered significant.

## Data availability

The data that support the findings of this study are available from the corresponding author upon reasonable request. The GenBank IDs of the constructed gene expression sequences were listed below: mRNA_KV1 (PV871909), mRNA_KV2 (PV871910), mRNA_KV3 (PV871911), mRNA_EV1 (PV871912), mRNA_EV2 (PV871913), mRNA_EV3 (PV871914), mRNA_SV1 (PV871915), mRNA_SV2 (PV871916).

Received: 9 July 2025; Accepted: 6 December 2025;
Published online: 31 December 2025

## References

1. Muteeb, G., Rehman, M. T., Shahwan, M. & Aatif, M. Origin of antibiotics and antibiotic resistance, and their impacts on drug development: a narrative review. *Pharmaceuticals* **16**, https://doi.org/10.3390/ph16111615 (2023).
2. Walsh, T. R., Gales, A. C., Laxminarayan, R. & Dodd, P. C. Antimicrobial resistance: addressing a global threat to humanity. *PLoS Med* **20**, e1004264 (2023).
3. Mirzayev, F. et al. World Health Organization recommendations on the treatment of drug-resistant tuberculosis, 2020 update. *Eur. Respir. J.* https://doi.org/10.1183/13993003.03300-2020 (2021).
4. Yin, Q. et al. Ecological dynamics of Enterobacteriaceae in the human gut microbiome across global populations. *Nature Microbiology* **10**, https://doi.org/10.1038/s41564-024-01912-6 (2025).

5. Vo, Q. T. et al. Utilization of cumulative antibiograms for public health surveillance: trends in Escherichia coli and Klebsiella pneumoniae susceptibility, Massachusetts, 2008-2018. *Infect Control Hosp Epidemiol.* **42**, 169–175 (2021).
6. Letara, N. et al. Prevalence and patient related factors associated with Extended-Spectrum Beta-Lactamase producing Escherichia coli and Klebsiella pneumoniae carriage and infection among pediatric patients in Tanzania. *Sci Rep.* **11**, 22759 (2021).
7. Velazquez, E. M. et al. Endogenous Enterobacteriaceae underlie variation in susceptibility to Salmonella infection. *Nat. Microbiol.* **4**, 1057–1064 (2019).
8. Lopez-Siles, M., Corral-Lugo, A. & McConnell, M. J. Vaccines for multidrug resistant Gram negative bacteria: lessons from the past for guiding future success. *FEMS Microbiol. Rev.* **45**, https://doi.org/10.1093/femsre/fuaa054 (2021).
9. Osterloh, A. Vaccination against bacterial infections: challenges, progress, and new approaches with a focus on intracellular bacteria. *Vaccines* **10**, https://doi.org/10.3390/vaccines10050751 (2022).
10. Yeh, M. T. et al. Engineering the live-attenuated polio vaccine to prevent reversion to virulence. *Cell Host Microbe* **27**, 736–751. e738 (2020).
11. Higham, S. L. et al. Intranasal immunization with outer membrane vesicles (OMV) protects against airway colonization and systemic infection with Acinetobacter baumannii. *J. Infect.* **86**, 563–573 (2023).
12. Li, S., Liang, H., Zhao, S. H., Yang, X. Y. & Guo, Z. Recent progress in pneumococcal protein vaccines. *Front. Immunol.* **14**, 1278346 (2023).
13. Crump, J. A. & Oo, W. T. Salmonella Typhi Vi polysaccharide conjugate vaccine protects infants and children against typhoid fever. *Lancet* **398**, 643–644 (2021).
14. Bergstrom, C., Fischer, N. O., Kubicek-Sutherland, J. Z. & Stromberg, Z. R. mRNA vaccine platforms to prevent bacterial infections. *Trends Mol. Med.* **30**, 524–526 (2024).
15. Khlebnikova, A., Kirshina, A., Zakharova, N., Ivanov, R. & Reshetnikov, V. Current progress in the development of mRNA vaccines against bacterial infections. *Int. J. Mol. Sci.* **25**, https://doi.org/10.3390/ijms252313139 (2024).
16. Maruggi, G., Zhang, C., Li, J., Ulmer, J. B. & Yu, D. mRNA as a transformative technology for vaccine development to control infectious diseases. *Mol. Ther.* **27**, 757–772 (2019).
17. Li, W., Wang, C., Zhang, Y. & Lu, Y. Lipid nanocarrier-based mRNA therapy: challenges and promise for clinical transformation. *Small* **20**, e2310531 (2024).
18. Wang, X. et al. Strong immune responses and protection of PcrV and OprF-I mRNA vaccine candidates against Pseudomonas aeruginosa. *npj Vaccines* **8**, 76 (2023).
19. Alameh, M. G. et al. A multivalent mRNA-LNP vaccine protects against Clostridioides difficile infection. *Science* **386**, 69–75 (2024).
20. Pardi, N. & Krammer, F. mRNA vaccines for infectious diseases - advances, challenges and opportunities. *Nat. Rev. Drug Discov* **23**, 838–861 (2024).
21. Mir, S. & Mir, M. The mRNA vaccine, a swift warhead against a moving infectious disease target. *Expert Rev. Vaccines* **23**, 336–348 (2024).
22. Alshabrmi, F. M. et al. An in-silico investigation to design a multi-epitopes vaccine against multi-drug resistant Hafnia alvei. *Vaccines* **10**, https://doi.org/10.3390/vaccines10071127 (2022).
23. Rodrigues, M. X., Yang, Y., de Souza Meira, E. B. Jr., do Carmo Silva, J. & Bicalho, R. C. Development and evaluation of a new recombinant protein vaccine (YidR) against Klebsiella pneumoniae infection. *Vaccine* **38**, 4640–4648 (2020).
24. Tomazi, T. et al. Immunization with a novel recombinant protein (YidR) reduced the risk of clinical mastitis caused by Klebsiella spp. and decreased milk losses and culling risk after Escherichia coli infections. *J. Dairy Sci.* **104**, 4787–4802 (2021).
25. Huang, T. et al. mRNA-LNP vaccines combined with tPA signal sequence elicit strong protective immunity against Klebsiella pneumoniae. *mSphere* **10**, e0077524 (2025).
26. Jiang, Z., Kang, X., Song, Y., Zhou, X. & Yue, M. Identification and evaluation of novel antigen candidates against Salmonella pullorum infection using reverse vaccinology. *Vaccines* **11**, https://doi.org/10.3390/vaccines11040865 (2023).
27. Neznansky, A. & Opatowsky, Y. Expression, purification and crystallization of the phosphate-binding PstS protein from Pseudomonas aeruginosa. *Acta Crystallogr. F Struct. Biol. Commun.* **70**, 906–910 (2014).
28. Neznansky, A., Blus-Kadosh, I., Yerushalmi, G., Banin, E. & Opatowsky, Y. The Pseudomonas aeruginosa phosphate transport protein PstS plays a phosphate-independent role in biofilm formation. *FASEB J.* **28**, 5223–5233 (2014).
29. Navon-Venezia, S., Kondratyeva, K. & Carattoli, A. Klebsiella pneumoniae: a major worldwide source and shuttle for antibiotic resistance. *FEMS Microbiol. Rev.* **41**, 252–275 (2017).
30. Bournazos, S. & Ravetch, J. V. Fcgamma receptor function and the design of vaccination strategies. *Immunity* **47**, 224–233 (2017).
31. Rethi-Nagy, Z. et al. STABILON, a novel sequence motif that enhances the expression and accumulation of intracellular and secreted proteins. *Int. J. Mol. Sci.* **23**, https://doi.org/10.3390/ijms23158168 (2022).
32. Chorro, L. et al. Preclinical immunogenicity and efficacy of optimized O25b O-antigen glycoconjugates to prevent MDR ST131 E. coli infections. *Infect. Immun.* **90**, e0002222 (2022).
33. Lu, J. et al. Salmonella: infection mechanism and control strategies. *Microbiol. Res.* **292**, 128013 (2025).
34. Spragge, F. et al. Microbiome diversity protects against pathogens by nutrient blocking. *Science* **382**, eadj3502 (2023).
35. Pan, C., Yue, H., Zhu, L., Ma, G. H. & Wang, H. L. Prophylactic vaccine delivery systems against epidemic infectious diseases. *Adv. Drug Deliv Rev.* **176**, 113867 (2021).
36. Amani, S. A. & Lang, M. L. Bacteria that cause enteric diseases stimulate distinct humoral immune responses. *Front. Immunol*. **11**, https://doi.org/10.3389/fimmu.2020.565648 (2020).
37. Ali, A. et al. Recent advancement, immune responses, and mechanism of action of various vaccines against intracellular bacterial infections. *Life Sci*. **314**, https://doi.org/10.1016/j.lfs.2022.121332 (2023).
38. Lin, I. Y. C., Van, T. T. H. & Smooker, P. M. Live-attenuated bacterial vectors: tools for vaccine and therapeutic agent delivery. *Vaccines Basel* **3**, 940–972 (2015).
39. Papadatou, I., Tzovara, I. & Licciardi, P. V. The role of serotype-specific immunological memory in pneumococcal vaccination: current knowledge and future prospects. Vaccines Basel **7**, https://doi.org/10.3390/vaccines7010013 (2019).
40. Kumar, P. et al. Evaluating the compatibility of new recombinant protein antigens (Trivalent NRRV) with a mock pentavalent combination vaccine containing whole-cell pertussis: analytical and formulation challenges. *Vaccines* **12**, https://doi.org/10.3390/vaccines12060609 (2024).
41. Ireton, K., Gyanwali, G. C., Herath, T. U. B. & Lee, N. Exploitation of the host exocyst complex by bacterial pathogens. *Mol. Microbiol.* **120**, 32–44 (2023).
42. Follador, R. et al. The diversity of Klebsiella pneumoniae surface polysaccharides. *Microb Genom.* **2**, e000073 (2016).
43. Shafaghi, M. et al. Immunoinformatics-aided design of a new multi-epitope vaccine adjuvanted with domain 4 of pneumolysin against strains. *Bmc Bioinform*. **24**, https://doi.org/10.1186/s12859-023-05175-6 (2023).
44. Goetz, M., Thotathil, N., Zhao, Z. M. & Mitragotri, S. Vaccine adjuvants for infectious disease in the clinic. *Bioeng. Transl. Med.* **9**, https://doi.org/10.1002/btm2.10663 (2024).
45. Sterzenbach, U. et al. Engineered exosomes as vehicles for biologically active proteins. *Mol. Ther.* **25**, 1269–1278 (2017).
46. Banskota, S. et al. Engineered virus-like particles for efficient in vivo delivery of therapeutic proteins. *Cell* **185**, 250–265.e216 (2022).

47. Moreira de Gouveia, M. I., Bernalier-Donadille, A. & Jubelin, G. Enterobacteriaceae in the human gut: dynamics and ecological roles in health and disease. *Biology* **13**, https://doi.org/10.3390/biology13030142 (2024).
48. Chen, H., Ren, X., Xu, S., Zhang, D. & Han, T. Optimization of lipid nanoformulations for effective mRNA delivery. *Int. J. Nanomed.* **17**, 2893–2905 (2022).

## Acknowledgements

This research was funded by a Start-up grant from Nanjing Agricultural University (Grant No. 804090). This study was also supported by Nanjing Chengshi (TheraRNA) Biomedical Technology Co. Ltd.

## Author contributions

R.L.: investigation, data curation, formal analysis, methodology, writing—original draft. S.X.: conceptualization, formal analysis, writing—review and editing, project administration. S.L.: data curation, formal analysis, writing—original draft. M.X. and J.L.: methodology, data curation, formal analysis, writing—review and editing. A.W., W.L., L.Z., and K.R.: investigation, data curation. C.F. and Z.W.: methodology, data curation, formal analysis. T. H.: conceptualization, supervision, writing—review and editing, project administration. Y.C.: conceptualization, supervision, writing—review and editing, funding acquisition. All authors have read and agreed to the published version of the manuscript.

## Competing interests

S.X., S.L., M.X., J.L., A.W., W.L., L.Z., K.R., C.F., Z.W. and T.H. are full-time employees of Nanjing Chengshi (TheraRNA) Biomedical Technology Co. Ltd. Nanjing Chengshi (TheraRNA) Biomedical Technology Co. Ltd. has filed patent for *K. pneumoniae* mRNA vaccine, *E. coli* mRNA vaccine, and *Salmonella* mRNA vaccine, listing Tiyun Han, Shi Xu, Jing Li, Mengwei Xu, and Caiyi Fei as co-inventors.

## Additional information

**Supplementary information** The online version contains supplementary material available at https://doi.org/10.1038/s41541-025-01346-z.

**Correspondence** and requests for materials should be addressed to Tiyun Han or Yafei Cai.